ACS APPLIED MATERIALS & INTERFACES

Research Article

www.acsami.org

Comparative Study of Ether-Based Electrolytes for Application in Lithium–Sulfur Battery

Lorenzo Carbone,[†] Mallory Gobet,[‡] Jing Peng,[‡,§] Matthew Devany,[∥] Bruno Scrosati,[⊥] Steve Greenbaum,*[,‡] and Jusef Hassoun*[,†]

[†]Sapienza University of Rome, Chemistry Department, Piazzale Aldo Moro, 5, 00185, Rome, Italy

[‡]Department of Physics & Astronomy, Hunter College of the City University of New York, New York, New York 10065, United States

[§]Ph.D. Program in Chemistry, City University of New York, New York, New York 10016, United States

[∥]Department of Chemistry and Biochemistry, Hunter College of the City University of New York, New York, New York 10065, United States

[⊥]Elettrochimica ed Energia, Via di Priscilla, 22, 00199, Rome, Italy

Supporting Information

ABSTRACT: Herein, we report the characteristics of electrolytes using various ether-solvents with molecular composition $CH_3O[CH_2CH_2O]_nCH_3$, differing by chain length, and $LiCF_3SO_3$ as the lithium salt. The electrolytes, considered as suitable media for lithium–sulfur batteries, are characterized in terms of thermal properties (TGA, DSC), lithium ion conductivity, lithium interface stability, cyclic voltammetry, self-diffusion properties of the various components, and lithium transference number measured by NMR. Furthermore, the electrolytes are characterized in lithium cells using a sulfur–carbon composite cathode by galvanostatic charge–discharge tests. The results clearly evidence the influence of the solvent chain length on the species mobility within the electrolytes that directly affects the behavior in lithium sulfur cell. The results may effectively contribute to the progress of an efficient, high-energy lithium–sulfur battery.

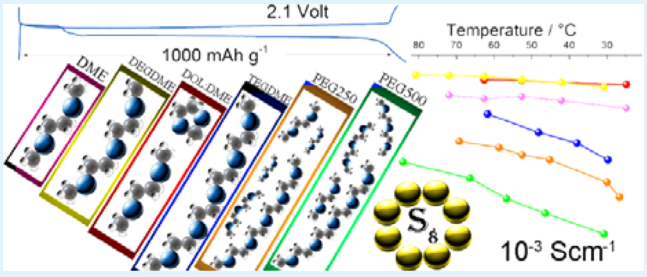

KEYWORDS: *lithium–sulfur battery, ether-based, glyme, electrolytes, NMR, diffusion*

INTRODUCTION

Recent development of the electrified mobility and renewable energy markets triggered increased demand for power supply improvements in hybrid electric vehicles (HEVs), plug-in hybrid vehicles (PHEVs), full electric vehicles (EVs), as well as for energy storage from renewable energy sources.[1] Lithium-ion battery, presently the most prevalent system for portable electronic devices, is considered the most promising candidate to satisfy the emerging market.[2] Improved safety, low cost and high energy content are the required parameters to be met for the large scale deployment of lithium-based energy storage systems.[3] Indeed, the present lithium battery is based on volatile organic carbonate electrolyte that leads to safety concerns associated with short-circuit and consequent risks of thermal runaway or fire evolution.[4] Ether-based electrolytes, in particular solutions using glymes and long chain $(-OCH_2CH_2-)_n$ solvents, represent an alternative, valid candidate characterized by low cost and high safety content.[5] Ethylene oxide unit, that is, $(-OCH_2CH_2-)$, is a Lewis base suitable for lithium salt solvation and consequent Li^+-ions motion that is, however, coordinated to polymer backbone or segment. Moreover, the strong interactions between mobile Li^+ specie and the ether oxygen atoms allow the ion–solvent coupled transport, that is, an easy process in low viscosity ether-based solvents that becomes more difficult in high viscosity or amorphous electrolytes and almost absent in crystalline solids.[6] Solid ether-based electrolytes, in particular polyethylene oxide (PEO), have shown favorable properties, in terms of good ionic conductivity,[7] satisfactory electrochemical and interfacial stability[8] and excellent mechanical properties,[9] however only at temperatures higher than 70 °C.[10] Polyethylene glycol dimethyl ether (PEGDME) and, in general members of the glyme-family, as well low molecular weight ethers may ensure good electrochemical properties at lower temperatures in comparison to PEO, thus allowing efficient use in lithium-ion, lithium-sulfur and lithium–air batteries.[11] In this work, we investigated the characteristics of electrolytes based on glyme solvents of various molecular weight, beginning from the analysis of the monomeric units (1,2-dimethoxyethane) DME, to poly-glyme of higher molecular weights (PEG500DME) using lithium trifluoromethansulfonate ($LiCF_3SO_3$) salt. Thermal, physical, and electrochemical properties of the

Received: March 11, 2015
Accepted: June 9, 2015
Published: June 9, 2015

DOI: 10.1021/acsami.5b02160
ACS Appl. Mater. Interfaces 2015, 7, 13859–13865

electrolytes were studied and following evaluated in lithium-sulfur cell.

EXPERIMENTAL SECTION

Electrolyte Preparation and Characterization. Before mixing, the solvents were dried for several days under molecular sieves until the water content was below 10 ppm as determined by 831 Karl Fisher Coulometer—METROHM. A schematic figure reporting the procedure used to lower the water content within the electrolytes is shown in the Supporting Information Figure S2. The electrolyte solutions were prepared by dissolving lithium trifluoromethanesulfonate ($LiCF_3SO_3$, that is, lithium triflate) in 1 mol kg^{-1} ratio in an argon filled glovebox. Lithium nitrate ($LiNO_3$) was then added to the solution in a 0.4 molar ratio. The prepared electrolytes are listed in Table 1

Table 1. List of Solvents and Salts with Corresponding Acronyms Used for the Electrolyte Characterized within This Study

electrolyte	salt	acronym
1,2-dimethoxyethane	$LiCF_3SO_3$; 1 mol kg^{-1}	DME
1,2-dimethoxyethane + 1,3-dioxolane (1:1 w/w)	$LiCF_3SO_3$; 1 mol kg^{-1}	DOL/DME
diethylene glycol dimethyl ether	$LiCF_3SO_3$; 1 mol kg^{-1} ratio	DEGDME
poly(ethylene glycol)$_4$ dimethyl ether	$LiCF_3SO_3$; 1 mol kg^{-1}	TEGDME
poly(ethylene glycol)$_n$ dimethyl ether $M_w \approx 250$	$LiCF_3SO_3$; 1 mol kg^{-1}	PEG250
poly(ethylene glycol)$_n$ dimethyl ether $M_w \approx 500$	$LiCF_3SO_3$; 1 mol kg^{-1}	PEG500

The thermal characterization was performed by thermogravimetric analysis TGA (Mattler Toledo TGA/SDTA851) and by differential scanning calorimetry DSC (Mattler Toledo DSC821). TGA was performed by raising the temperature from 25 to 700 °C, with a heat rate of 10 °C/min. DSC was performed by cooling from 25 °C to −80 °C at −5 °C/min. Conductivity tests were performed by using 2032 coin cells including stainless steel symmetrical electrodes and Teflon O-ring separator with a constant and known size to ensure a fixed cell constant. Electrochemical impedance spectroscopy (EIS) was performed by using a VSP (Biologic) instrument with 10 mV-signal amplitude, within 500 MHz-100 Hz frequency range. The interface resistance has been calculated by nonlinear least-squares (NLLSQ) fit of the impedance spectra, carried out by using a Boukamp software product. An $R(RQ)nQ$ equivalent circuit was used for the Nyquist plot analysis, where R represents a resistance and Q a constant-phase element (CPE). The chi-square (χ^2), a parameter used to evaluate the fitting quality, was below 10^{-4}.[12,13] An example of interface resistance represented by Nyquist plot of the EIS data is reported in the Supporting Information Section, Figure S1).The electrochemical stability window was studied by linear sweep voltammetry (LSV) at a scan rate of 0.1 mV s^{-1}, in a three electrodes lithium cell using a VSP (Biologic) instrument. The cell configuration consisted of lithium metal as counter and reference electrode and super P on aluminum as working electrode and the measurement was performed within OCV−5.0 V vs Li/Li^+ range at room temperature. Temperature dependence of the self-diffusion coefficient for ^1H, ^{19}F, and ^7Li nuclei was measured on a Bruker 400 Avance III NMR spectrometer using a double stimulated echo pulse sequence to suppress convection effects.[14] Gradient pulses, of sine shape with duration δ = 2−5 ms and strength g = 0−45 G/cm, were applied with a diffusion delay of Δ = 80−800 ms within a temperature ranging 20 and 70 °C, in steps of 10 °C. The self-diffusion activation energies were estimated by the Arrhenius plot linear slope of the corresponding self-diffusion coefficients measured at various temperatures. The room temperature lithium transference number (t^+), corresponding to the fraction of current carried = by the lithium ions, was determined as the ratio of the self-diffusion coefficient of Li^+ with respect to overall charge carriers, that is, Li^+ (^7Li nuclei) and $CF_3SO_3^-$ (^{19}F nuclei) measured at 25 °C. This method does not take into account the effects of ion association and is therefore used only as guide to comparative behavior in electrolytes.

Lithium stripping/deposition galvanostatic test was performed by applying a 0.1 mA cm^{-2} current to Li/Li symmetrical cell, using a MACCOR Series 4000 Battery Test System (Maccor Inc.).

Cathode Preparation and Test in Lithium−Sulfur Cell. The cathode material was based on elemental sulfur and mesophase micro bead (MCMB) carbon, in a weight ratio of 1:1. Before mixing with MCMB, the sulfur was heated to 135 °C, until completely melted. The mixture was stirred for 3 h at 135 °C and then cooled down to room temperature. A stainless steel jar was used to hold and mechanically treat the sample by high-energy ball milling system (Retsch Mill MM400) with a frequency of 15 Hz for a total time of 2 h, using a milling time of 30 min, rest period of 15 min and repeating the above procedure four times.

The electrodes were prepared by mixing the carbon−sulfur composite, super P carbon (Timcal) and polyvinylidinedifluoride (PVDF) binder in 80:10:10 mass ratio in *N*-methylpyrrolidone (NMP) solution. The slurry was coated using Doctor Blade technique on aluminum foil current collector, punched as disks and then vacuum-dried at 50 °C for 24 h before assembling the cells. The galvanostatic tests were performed in lithium half-cells, using a separator soaked with 30 μL of electrolyte. Cycling tests were performed using a Maccor

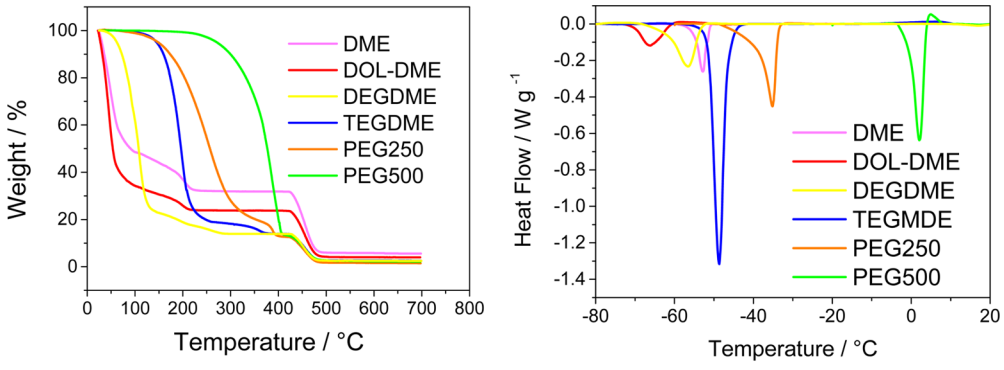

(A) (B)

Figure 1. (A) Thermogravimetric analysis (TGA) profiles of the ether-based electrolytes performed from 25 °C to 700 °C at 10 °C/min heating rate, under nitrogen flow. (B) Differential scanning calorimetry (DSC) profiles of the ether-based electrolytes cooled from 20 to −80 °C at 5 °C/min, under argon atmosphere.

DOI: 10.1021/acsami.5b02160
ACS Appl. Mater. Interfaces 2015, 7, 13859−13865

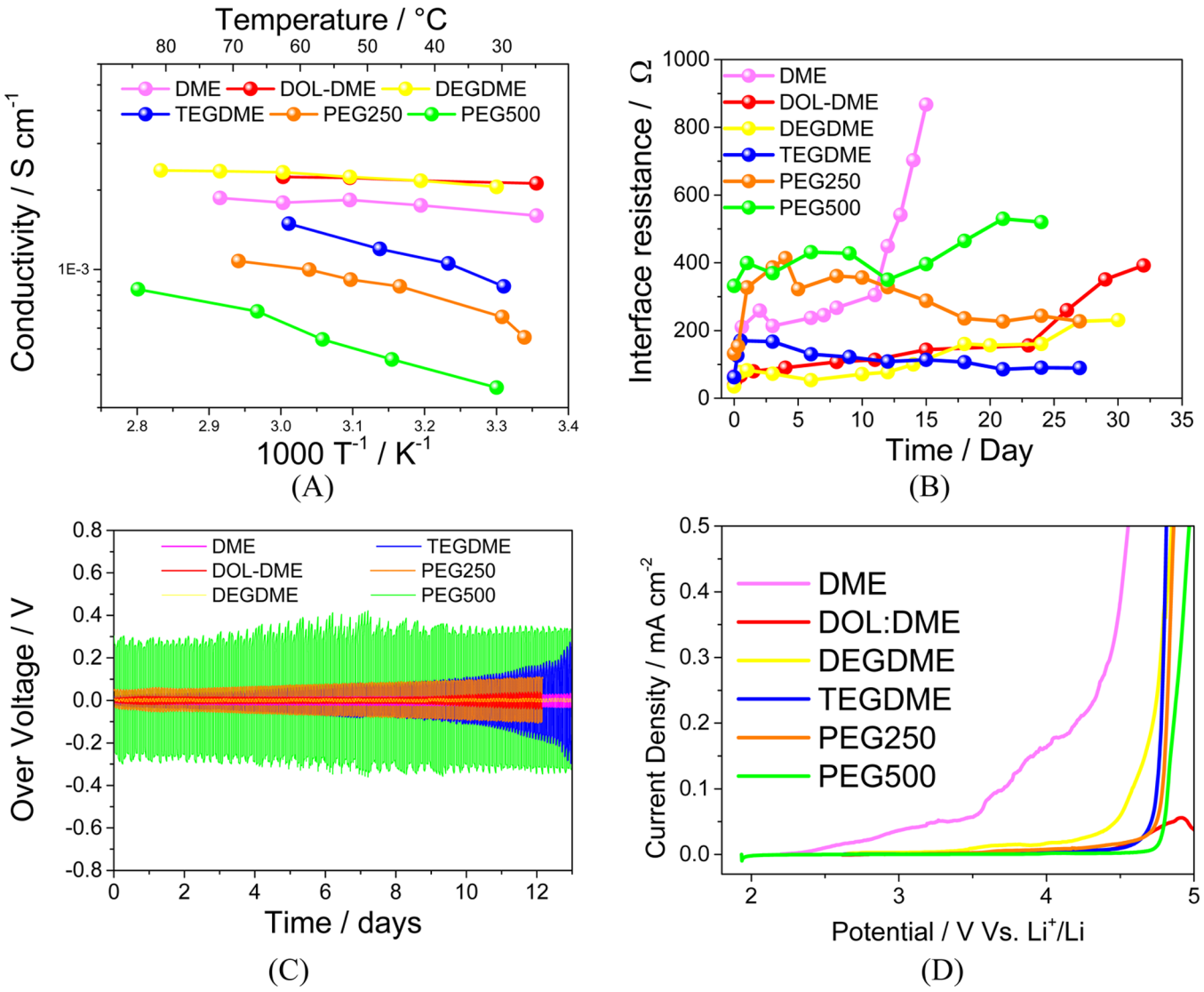

Figure 2. (A) Conductivity Arrhenius plots of the ether-based electrolytes performed by varying the temperature from 30 to 80 °C. The measurements have been performed in a coin-cell, using electrochemical impedance spectroscopy with signal amplitude of 10 mV within 500 MHz−100 Hz frequency range. (B) Time evolution at room temperature of the lithium-electrolyte interface resistance performed in Swagelok-type, Li/Li symmetrical cell using electrochemical impedance spectroscopy with signal amplitude of 10 mV within 500 MHz−100 mHz frequency range. (C) Voltage versus time profile of lithium deposition/stripping galvanostatic test performed applying a 0.1 mA cm^{-1} current to symmetrical Li/electrolyte/Li cell. (D) Current vs potential profile of the linear sweep voltammetry (LSV) performed using the Li/electrolyte/SP cell within the OCV−5.0 V vs Li/Li^+ range at 0.1 mV s^{-1} and room temperature employed for the determination of the electrochemical stability window of the electrolyte.

instrument at a C/20 current rate (1C = 1675 mA g^{-1} based on the sulfur weight), within 1−3.2 V limit.

RESULT AND DISCUSSION

Thermogravimetric analysis (TGA) was performed to detect the stability of the various ether-based electrolytes at elevated temperature. The DSC and, in particular, the TGA measurement are considered as an indication of the upper and lower temperature limits where the electrolytes maintain their characteristics. Therefore, we used this information as a suggested temperature range suitable for stable working of the cell. Figure 1A, reporting the TGA traces, demonstrates that the electrolytes based on both DME and DOL-DME are characterized by thermal stability limited to temperatures lower than 50 °C, while DEG-based one reveals a slightly higher stability, that is, extended up to 70 °C. In contrast, TEG-based electrolyte shows a thermal stability exceeding 200 °C that is further increased for PEG500-based one up to a temperature as high as 350 °C. As indeed expected, the above results reflect a thermal stability enhanced by the increasing the ether-chain length, that is, DOL-DME < DEG < PEG250 < PEG500, thus suggesting a higher safety content of the long-chain, ether-based electrolytes in view of the possible application in lithium batteries. The DSC measurements performed within the electrolyte crystallization region, and reported in Figure 1B, indicate a lower freezing point for DME and DOL-DME-based electrolytes, that is, of about −53 and −68 °C, respectively, in respect to TEGDME and PEG250-based electrolytes that show the still very low freezing points of −49 and −34 °C, respectively. PEG500-based electrolyte freezes at about 5 °C, thus suggesting possible issues associated with its use at the lower temperatures.

DOI: 10.1021/acsami.5b02160
ACS Appl. Mater. Interfaces 2015, 7, 13859−13865

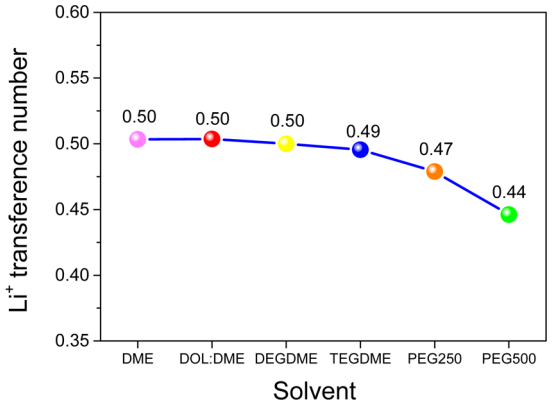

Figure 3. Lithium transference number of the ether-based electrolytes at room temperature. The *values* have been *obtained* as the ratio of the self-diffusion coefficient of Li^+ with respect to that of overall charge carriers, that is, Li^+ and $CF_3SO_3^-$ measured at 25 °C by NMR.

Figure 2A, reporting the conductivity Arrhenius plots of the selected electrolytes, shows conductivity values suitable for lithium battery applications for all the samples in the studied temperature range. Indeed, the room temperature conductivity decreases from about 2×10^{-3} S cm^{-1} for DME, DOL/DME, and DEGDME-based electrolytes to about 1×10^{-3} for TEGDME, 7×10^{-4} for PEG250, and down to 4×10^{-4} S cm^{-1} for PEG500-based one, thus suggesting increasing conductivity by decreasing the ether-chain length. However, DME and DEGDME show a different trend, most likely because of an additional effect of the solvent dielectric constant that is predominant at the low viscosity values. Indeed, DME has a lower viscosity, as well as a lower dielectric constant than DEGDME (i.e., 0.46 mPa·s and 5.5, respectively, for DME and 1.03 mPa·s and 5.8, respectively, for DEGDME).[15] This is reflected by a slightly lower conductivity of the former with respect to the latter. Furthermore, a slight and linear increase of the conductivity, in particular for the electrolyte based on PEG500, is observed by raising the temperature as also expected by solvent viscosity decrease. The time evolution of the lithium interface resistance of the symmetrical lithium cells using the studied electrolytes reported in Figure 2B reveals a stable lithium-electrolyte interface, with relatively low resistance ranging from 100 Ohm for DOL-DME, DEGDME, and TEGDME-based solutions to 400 Ohm for PEG250 and PEG500-based ones. However, the cell using DME-based electrolyte shows a continuous increase of the interface resistance because of possible evaporation over time, thus excluding its possible use as the electrolyte solvent for lithium battery applications, while DOL-DME combination appears a still suitable solution. DEGDME and TEGDME-based

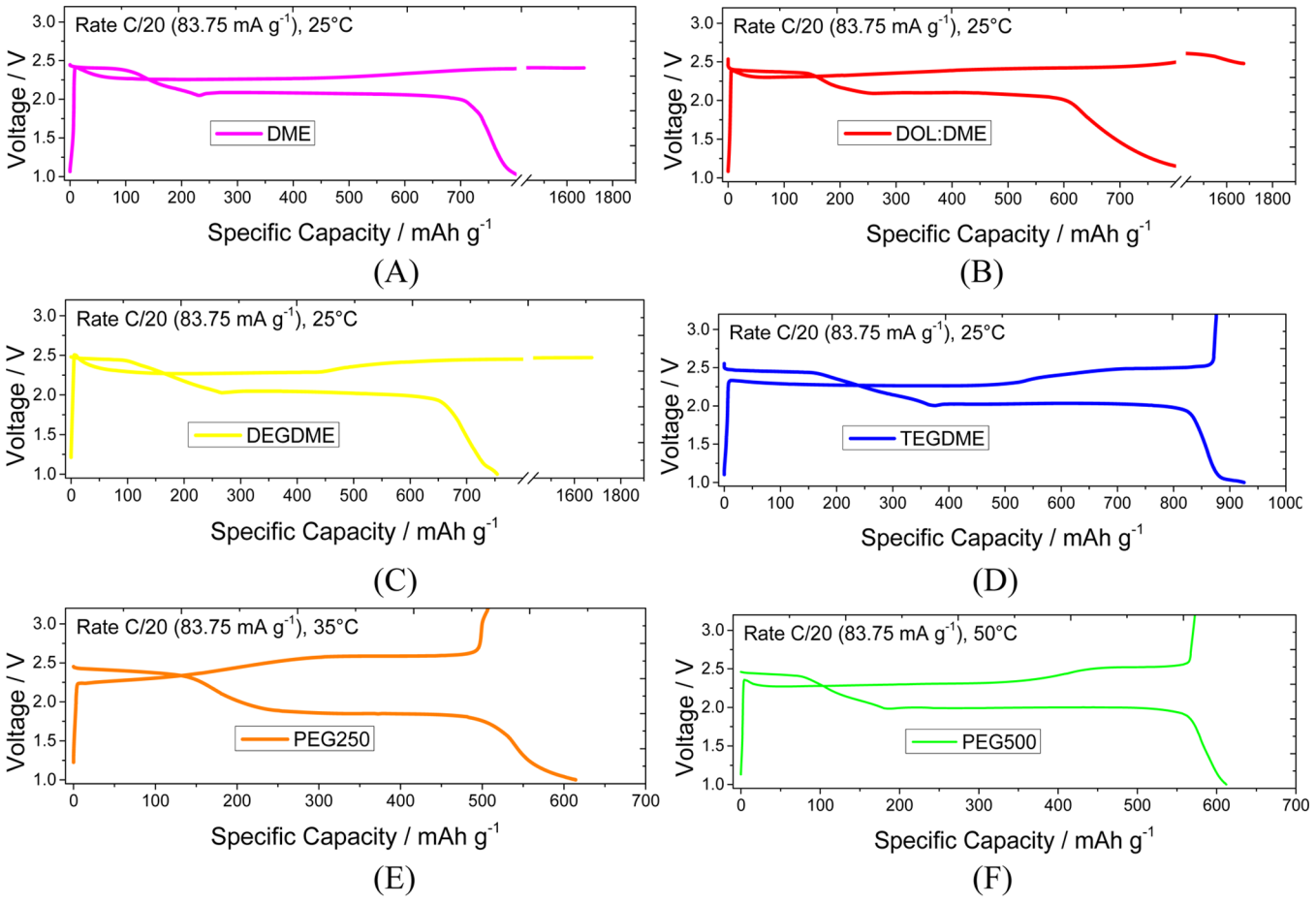

Figure 4. Voltage profile of the lithium sulfur cells using the various electrolytes, that is, (A) DME-1m $LiCF_3SO_3$ at 25 °C, (B) DEGDME-1m $LiCF_3SO_3$ at 25 °C, (C) DOL-DME-1m $LiCF_3SO_3$ at25 °C (D) TEGDME 1m $LiCF_3SO_3$ at 25 °C, (E) PEG250−1m $LiCF_3SO_3$ at 35 °C, and (F) PEG500−1m $LiCF_3SO_3$ at 50 °C. The galvanostatic charge−discharge cycle is performed at a current rate of C/20 (83.75 mA g^{-1}) within 1.2−3.2 V voltage.

DOI: 10.1021/acsami.5b02160
ACS Appl. Mater. Interfaces 2015, 7, 13859−13865

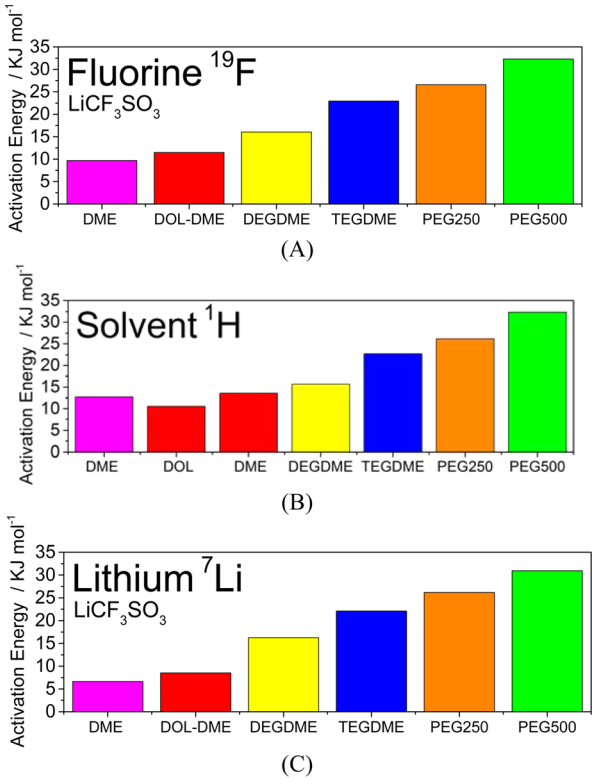

Figure 5. Comparison of self-diffusion activation energy for ^{19}F (A), ^{1}H (B), and ^{7}Li (C) nuclei.

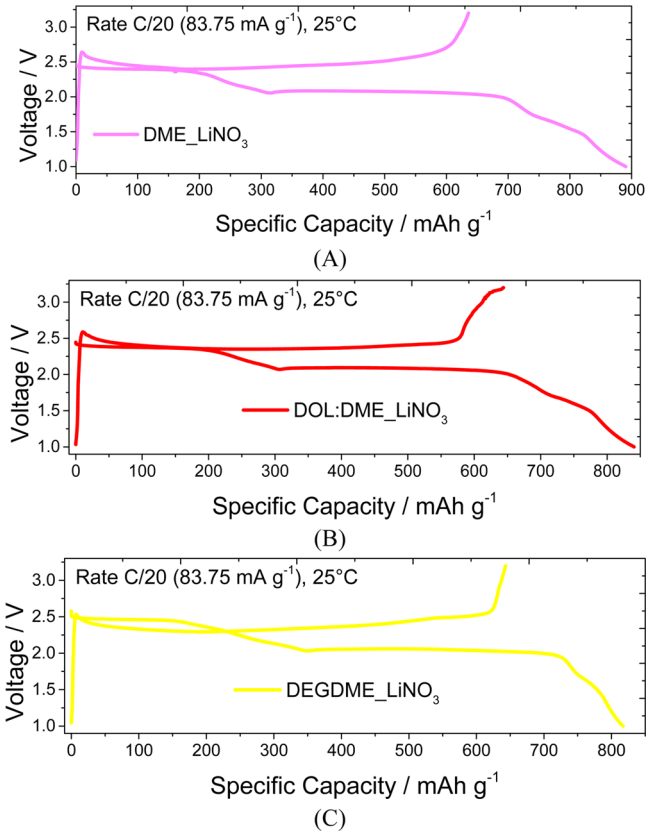

Figure 6. Voltage profiles of the galvanostatic charge−discharge cycle of lithium sulfur cells using DME-1m $LiCF_3SO_3$ (A), DOL:DME-1m $LiCF_3SO_3$ (B), and DEGDME-1m $LiCF_3SO_3$ (C) electrolytes added with 0.4m $LiNO_3$ as lithium polysulfide shuttle protecting-agent. Current rate C/20 = 83.75 mA g^{-1}, voltage range 1.2−3.2 V. Room temperature.

solutions show lower resistance values and excellent stability over time, thus suggesting these electrolytes as the preferred ones for application in lithium cell. The lithium stripping-deposition voltage profiles shown in Figure 2C evidence a very limited overvoltage, that is, to about 10 mV, for DME and DEGDME-based electrolytes (pink and yellow curves, respectively) with an increase of the value by increasing the chain length to about 300 mV for PEG500-based electrolyte (green curve) at room temperature, which is most likely associated with the increased charge transfer resistance at the lithium interphase. Furthermore, minor changes in the polarization value, in particular for TEGDME-based electrolyte, is observed over time because of the expected growth and following consolidation of the solid electrolyte interphase (SEI) film at the lithium surface upon lithium stripping-deposition.[16,17] In line with the results already observed by time evolution test of the Li-interface resistance (see Figure 2B), the lithium deposition-stripping test suggests DEGDME as preferred electrolyte solvent for application in lithium battery. The linear sweep voltammetry (LSV) in lithium/carbon cells reported in Figure 2D exhibits the same trend for DEGDME, TEGDME, PEG250, and PEG500, with electrochemical stability extended up to 4.5 V.

In spite of the decomposition onset of DME-based electrolyte at about 2.5 V, the electrolyte obtained by DOL and DME combination shows rather higher stability, that is, extended up 4.0 V. This test, in addition to the previous ones (see Figure 2 A, B and C), suggest possible interactions between the two cosolvents, that is, DOL and DME, leading to a mixed phase with slightly different electrochemical properties with respect to the single solvent.

Lithium transference number plays a key role in optimizing the behavior of the electrolyte in Li-cell. This important parameter is here determined by using the ionic self-diffusion coefficients as determined by NMR (see experimental section for details) and reported in Figure 3.[18−20] Indeed, the figure shows a decrease of the lithium transference by increasing the ether-chain length from DME to PEG500-based electrolyte. The observed decrease of the lithium transference number may be most likely ascribed to the expected kinetic limits hindering the solvated-ions mobility by increasing the ether-chain length.[21,22]

Figure 4 shows the voltage profiles of the first galvanostatic charge−discharge cycle of the various electrolytes in a lithium−sulfur cell. The figure evidences a remarkable polysulfide-shuttle effect for the cells using short-chain glymes,[23] that is, DME (A), DEGDME (B), and DOL:DME (C), characterized by conventional discharge process and by continuous charging, until cell failure.[24] Instead, the cells using TEGDME (D), PEG250 (E), and PEG500 (F) reveal very limited, or complete absence of polysulfide-shuttle reaction during the first cycle, with a typical trend associated to the Li-sulfur process.[25] However, the performance of the sulfur cell using TEGDME, characterized by a capacity of about 900 mAh g^{-1} and limited polarization, may be approached only by raising the temperature up to 35 and 50 °C for the cell using PEG250 and PEG500, respectively. This behavior may be ascribed to the lower conductivity and higher viscosity of the long-chain glymes at room temperature, and consequent high activation

DOI: 10.1021/acsami.5b02160
ACS Appl. Mater. Interfaces 2015, 7, 13859−13865

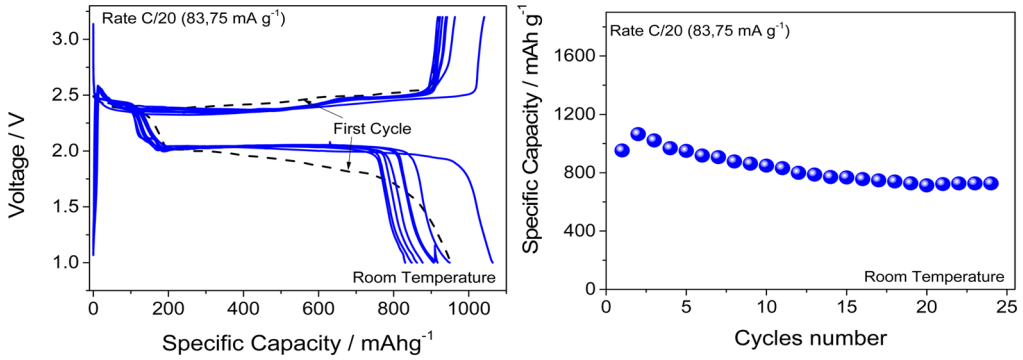

Figure 7. Galvanostatic behavior of a Li/DEGDME-$LiCF_3SO_3$–$LiNO_3$/S–C coin-cell reported in terms of voltage profile (A) and corresponding cycling behavior (B). Current rate C/20 = 83.75 mA g^{-1}, voltage range 1.2–3.2 V. Room temperature.

energy required for the motion of the various electrolyte constituents, in particular at the electrode–electrolyte interface.

Furthermore, the cell using TEGDME shows higher capacity than that using DEGDME, despite the lower viscosity of the latter. This aspect may be reasonably attributed to the lower resistance observed in Figure 2B for the Li-TEGDME interface with respect to Li-DEGDME, however further study is required to fully clarify this trend.

Figure 5 reports the self-diffusion activation energies of the various species within the electrolytes obtained by Arrhenius plot linear-slope determination of the self-diffusion coefficient for ^{1}H, ^{19}F, and ^{7}Li nuclei measured by NMR (see Experimental Section for details).

The ^{19}F (Figure 5A) and ^{7}Li (Figure 5C) self-diffusion activation energies are ascribed to the $LiCF_3SO_3$ salt ions moving within the selected solvent, while the ^{1}H activation energy (Figure 5B) is associated with the ether-segment diffusion. The figure shows that the short-chain glymes are generally characterized by lower activation energy in comparison to the long chain ethers. Indeed, DOL and DME-based electrolytes reveal very low activation energy both of the salt and of the ether-chains, that is, ranging from 5 to 10 kJ mol^{-1}, hence a higher mobility in respect to PEG-based electrolytes, characterized by an activation energy ranging from 25 to about 30 kJ mol^{-1}. DEGDME and TEGDME-based solutions exhibit intermediate values, that is, ranging from 15 to 20 kJ mol^{-1}. The similarity in values and activation energy trends between the ions and the host molecules is consistent with the highly cooperative ion transport mechanism known to occur in ether-based solvents. The above-reported data are in line with the remarkable shuttle reaction observed in Figure 4 (A, B, and C) for lithium sulfur cells using electrolyte based on short-chain glymes, in which the high mobility of salt ions and solvents allows an easy pathway for polysulfide migration from cathode to anode, and consequent direct reaction. Instead, long-chain glymes partially inhibit the above process that is almost absent during the first charge–discharge of the corresponding Li–S cells (see Figure 4 D, E and F). It is worth noting that the above polysulfide shuttle effect in short-chain glymes may be efficiently mitigated by protecting the lithium electrode surface, such as by adding lithium nitrate ($LiNO_3$) salt to the electrolyte solution.[26,27]

Accordingly, Figure 6 reporting the voltage profile of the cells using DME (A), DOL:DME (B), and DEGDME (C) solutions, with added $LiNO_3$, clearly evidence the reduction of the polysulfide shuttle-effect, and the corresponding increase of the cell efficiency during the galvanostatic charge–discharge cycle. Furthermore, the figure shows an over discharge at about 1 V, attributed to the $LiNO_3$ reduction, significantly buffering the lithium polysulfide shuttle reaction. The figure shows the typical profile expected for the Li–S reaction and a relatively limited polarization. These data, in addition to the previous experimental evidence, suggest DEGDME-$LiCF_3SO_3$ with added $LiNO_3$ solution is a suitable medium for application in lithium–sulfur cell.

Therefore, DEGDME-$LiCF_3SO_3$–$LiNO_3$ solution has been employed as the electrolyte in Li/S cell, of coin-configuration, galvanostatically cycled for several times at C/20 rate, that is, a low current to evaluate possible shuttle process, in general magnified at the lower C-rates. The results in Figure 7, reported in terms of voltage profile (A) and corresponding cycling behavior (B), confirm the mitigation of this side reaction by showing a Coulombic efficiency higher than 90%. The figure reveals an initial capacity of about 900 mAh g^{-1} due to the reversible Li–S reaction, that decreases and then stabilizes at about 750 mAh g^{-1} because of polysulfide dissolution until final solution saturation. The above saturation, with consequent buffer-effect by mass action of the dissolved polysulfide, avoids further cathode loss and leads to capacity stabilization. This is also favored by the use of a separator soaked by a very low electrolyte amount, that is, about 10–15 μL. Taking into account a specific capacity of about 750 mAh g^{-1} and a working voltage of 2 V, the theoretical energy of the cell may be calculated to be of the order of 1500 Wh kg^{-1} that may reflect, considering side and inactive cell components, a practical energy as high as 500 Wh kg^{-1} and, finally, of 250 Wh kg^{-1} considering also the carbon content of the sulfur electrode employed for the tests (i.e., S:C, 1:1 weight ratio)

CONCLUSION

Various electrolytes differing by concepts, design, and materials, as well as the effect of their chemical and physical characteristics on the lithium–sulfur battery performance, have been recently reviewed.[28] Herein, we focused our attention on the species mobility within glyme-based electrolytes and its effects on the polysulfide shuttle reaction. We studied the characteristics of ether-based solutions differing by chain-length as suitable electrolyte media for lithium–sulfur cell. The properties of the electrolytes have been investigated by combining electrochemical and NMR techniques. The results suggest that the

DOI: 10.1021/acsami.5b02160
ACS Appl. Mater. Interfaces 2015, 7, 13859–13865

mobility of the various species within the electrolyte, such as lithium salt ions, solvent and polysulfide, is strongly affected by the ether chain-length and directly reflected in the behavior of the corresponding Li−S cell. Long-chain glymes show low species mobility reflecting in lower conductivity and, simultaneously, less pronounced polysulfide-shuttle reaction in comparison to short-chain glymes. On the other hand, the polysulfide-shuttle has been efficiently mitigated in short-chain glyme, that is, DEGDME-$LiCF_3SO_3$, by adding $LiNO_3$ salt to the solution, thus leading to a Li−S cell characterized by a stable capacity of 750 mAh g^{-1} and an expected practical energy higher than 250 Wh kg^{-1}.

■ ASSOCIATED CONTENT

Supporting Information

Interface resistance trend and procedure used to lower the water content within the electrolytes. The Supporting Information is available free of charge on the ACS Publications website at DOI: 10.1021/acsami.5b02160.

■ AUTHOR INFORMATION

Corresponding Authors

*E-mail: steve.greenbaum@hunter.cuny.edu.
*E-mail: Jusef.hassoun@uniroma1.it.

Notes

The authors declare no competing financial interest.

■ ACKNOWLEDGMENTS

The work at Hunter College was supported by a grant from the U.S. Office of Naval Research, and the Hunter NMR facility is funded by a National Institutes of Health RCMI infrastructure grant (RR 003037).

■ REFERENCES

(1) Kang, B.; Ceder, G. Battery Materials for Ultrafast Charging and Discharging. *Nature* **2009**, *458*, 190−193.
(2) Tarascon, J. M.; Armand, M. Issues and Challenges Facing Rechargeable Lithium Batteries. *Nature* **2001**, *414*, 359−367.
(3) Scrosati, B.; Garche, J. Lithium Batteries: Status, Prospects and Future. *J. Power Sources* **2010**, *195*, 2419−2430.
(4) Wang, Q.; Ping, P.; Zhao, X.; Chu, G.; Sun, J.; Chen, C. Thermal Runaway Caused Fire and Explosion of Lithium Ion Battery. *J. Power Sources* **2012**, *208*, 210−224.
(5) Marmorstein, D.; Yu, T. H.; Striebel, K. A.; McLarnon, F. R.; Hou, J.; Cairns, E. J. Electrochemical Performance of Lithium Sulfur Cells with Three Different Polymer Electrolytes. *J. Power Sources* **2000**, *89*, 219−226.
(6) Xiong, H. M.; Zhao, K.; Zhao, X.; Wang, Y.; Chen, J. S. Elucidating the Conductivity Enhancement Effect of Nano-Sized SnO_2 Fillers in the Hybrid Polymer Electrolyte PEO−SnO_2−$LiClO_4$. *Solid State Ionics* **2003**, *159*, 89−95.
(7) Zewde, B. W.; Admassie, S.; Zimmermann, J.; Isfort, C. S.; Scrosati, B.; Hassoun, J. Enhanced Lithium Battery with Polyethylene Oxide-Based Electrolyte Containing Silane−Al_2O_3 Ceramic Filler. *ChemSusChem* **2013**, *6*, 1400−1405.
(8) Zewde, B. W.; Elia, G. A.; Admassie, S.; Zimmermann, J.; Hagemann, M.; Isfort, C. S.; Scrosati, B.; Hassoun, J. Polyethylene Oxide Electrolyte Added by Silane-Functionalized TiO_2 Filler for Lithium Battery. *Solid State Ionics* **2014**, *268*, 174−178.
(9) Appetecchi, G. B.; Hassoun, J.; Scrosati, B.; Croce, F.; Cassel, F.; Salomon, M. Hot-Pressed, Solvent-Free, Nano-Composite, PEO-Based Electrolyte Membranes II. All Solid-State Li/$LiFePO_4$ Polymer Batteries. *J. Power Sources* **2003**, *124*, 246−253.
(10) Croce, F.; Appetecchi, G. B.; Persi, L.; Scrosati, B. Nano-Composite Polymer Electrolytes for Lithium Batteries. *Nature* **1998**, *394*, 456−458.
(11) Henderson, W. A. Glyme−Lithium Salt Phase Behavior. *J. Phys. Chem. B* **2006**, *110*, 13177−13183.
(12) Boukamp, B. A. A Package for Impedance/Admittance Data Analysis. *Solid State Ionics* **1986**, *18*, 136−140.
(13) Boukamp, B. A. A Nonlinear Least Squares Fit Procedure for Analysis of Immittance Data of Electrochemical Systems. *Solid State Ionics* **1986**, *20*, 31−44.
(14) Jerschow, A.; Müller, N. Suppression of Convection Artifacts in Stimulated-echo Diffusion Experiments. Double-Stimulated-Echo Experiments. *J. Magn. Reson.* **1997**, *125*, 372−375.
(15) Chrétien, F.; Jones, J.; Damas, C.; Lemordant, D.; Willmann, P.; Anouti, M. Impact of Solid Electrolyte Interphase Lithium Salts on Cycling Ability of Li-Ion Battery: Beneficial Effect of Glymes Additives. *J. Power Sources* **2014**, *248*, 969−977.
(16) Bernhard, R.; Latini, A.; Panero, S.; Scrosati, B.; Hassoun. Poly(Ethyleneglycol) Dimethylether Lithium Bis-(trifluoromethanesulfonyl)imide, PEG500DMEeLiTFSI, as High Viscosity Electrolyte for Lithium Ion Batteries. *J. Power Sources* **2013**, *226*, 329−333.
(17) Elia, G. A.; Bernhard, R.; Hassoun, J. A Lithium-Ion Oxygen Battery Using a Polyethylene Glyme Electrolyte Mixed With an Ionic Liquid. *RSC Adv.* **2015**, *5*, 21360−21365.
(18) Fromling, T.; Kunze, M.; Schonhoff, M.; Sundermeyer, J.; Roling, B. Enhanced Lithium Transference Numbers in Ionic Liquid Electrolytes. *J. Phys. Chem. B* **2008**, *112*, 12985−12990.
(19) Zugmann, S.; Fleischmann, M.; Amereller, M.; Gschwind, R. M.; Wiemhöfer, H. D.; Gores, H. J. Measurement of Transference Numbers for Lithium ion Electrolytes Via Four Different Methods, A Comparative Study. *Electrochim. Acta* **2011**, *56*, 3926−3933.
(20) Saito, Y.; Yamamoto, H.; Nakamura, O.; Kageyama, H.; Ishikawa, H.; Miyoshi, T.; Matsuoka, M. Determination of Ionic Self-Diffusion Coefficients of Lithium Electrolytes Using the Pulsed Field Gradient NMR. *J. Power Sources* **1999**, *81*−*82*, 772−776.
(21) Lee, D. J.; Agostini, M.; Park, J. W.; Sun, Y. K.; Hassoun, J.; Scrosati, B. Progress in Lithium−Sulfur Batteries: The Effective Role of a Polysulfide-Added Electrolyte as Buffer to Prevent Cathode Dissolution. *ChemSusChem* **2013**, *6*, 2245−2248.
(22) Elia, G. A.; Park, J. B.; Sun, Y. K.; Scrosati, B.; Hassoun, J. Role of the Lithium Salt in the Performance of Lithium−Oxygen Batteries: A Comparative Study. *ChemElectroChem.* **2014**, *1*, 47−50.
(23) Yuriy, V.; Mikhaylik, Z.; Akridge, J. R. Polysulfide Shuttle Study in the LiOS Battery System. *J. Electrochem. Soc.* **2004**, *151*, 1969−1976.
(24) Bruce, P. G.; Freunberger, S. A.; Hardwick, L. J.; Tarascon, J. M. $Li-O_2$ and Li−S Batteries with High Energy Storage. *Nat. Mater.* **2012**, *11*, 19−29.
(25) Zhang, S. S. Liquid Electrolyte Lithium/Sulfur Battery: Fundamental Chemistry, Problems, and Solutions. *J. Power Sources* **2013**, *231*, 153−162.
(26) Agostini, M.; Lee, D. J.; Scrosati, B.; Sun, Y. K.; Hassoun, J. characteristics of Li_2S_8-Tetraglyme Catholyte in a Semi-Liquid Lithium Sulfur Battery. *J. Power Sources* **2014**, *265*, 14−19.
(27) Aurbach, D.; Pollak, E.; Elazari, R.; Salitra, G.; Kelley, C. S.; Affinito, J. On the Surface Chemical Aspects of Very High Energy Density, Rechargeable Li−Sulfur Batteries. *J. Electrochem. Soc.* **2009**, *156*, 694−702.
(28) Scheers, J.; Fantini, S.; Johansson, P. A Review of Electrolytes for Lithium-Sulphur Batteries. *J. Power Sources* **2014**, *255*, 204−218.

DOI: 10.1021/acsami.5b02160
ACS Appl. Mater. Interfaces 2015, 7, 13859−13865